ACS OMEGA

Open Access

http://pubs.acs.org/journal/acsodf

Article

Design and Synthesis of a Polyketone Building Block with Vinyl Groups—9,10-Diethyl-9,10-ethenoanthracene-2,3,6,7(9*H*,10*H*)-tetraone—and a Preliminary Photoelectrical Property Study of Its Azaacene Derivatives

Hong Chen, Shilong Zhang, Jinlei Liu, Jiaxin Li, Wangqiao Chen,* and Guofu Zhou*

Cite This: *ACS Omega* 2023, 8, 32931−32939

Read Online

ACCESS | Metrics & More | Article Recommendations | Supporting Information

ABSTRACT: Polyketone compounds are powerful building blocks to synthesize various organic functional materials. Despite that a great many number of planar and non-planar polyketone building blocks have been developed, one issue is that generally there are only ketone functional groups on the molecular skeleton, which will constrain their transformation and further limit the development of functional materials. In this work, we report the design and synthesis of a building block 9,10-diethyl-9,10-ethenoanthracene-2,3,6,7(9*H*,10*H*)-tetraone with additional vinyl functional groups. In addition, its azaacene derivatives were also synthesized, and their preliminary physicochemical properties were studied.

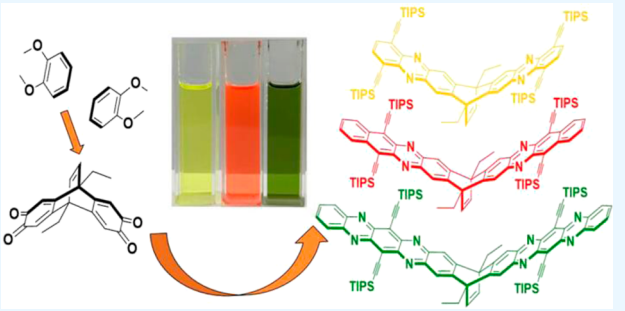

INTRODUCTION

Compounds with polyketone functional groups are important building blocks and can transform into many other different types of organic functional materials, including polyaromatic hydrocarbons (PAHs),[1] N-doped polyaromatic hydrocarbons (N-PAHs),[2] covalent organic frameworks (COFs),[3] etc. As shown in Figure 1, the previously reported polyketone building blocks can be generally classified into two groups: planar and non-planar.

For the planar polyketone building blocks, compounds **1** and **2** were synthesized efficiently in 2005 through ruthenium(III) chloride-catalyzed oxidation[4] and were further demonstrated as powerful building blocks to synthesize various PAH and N-PAH derivatives, including nonatwistarene (9-PAH),[5] dodecatwistarene (12-PAH),[6] as well as N-doped dodecatwistarene (12-N-PAH)[7] reported by Zhang's group and 11-N-PAH,[8] 18-N-PAH,[9] and 53-N-PAH[10] reported by Mastalerz's group, Baumgarten's group, and Mateo-Alonso's group, respectively. In addition, they were also important units to build COF materials. Briefly, to name some examples, Jiang's group used compounds **3** and **2** to synthesize FAN-24 (FAN = fused aromatic network; FAN[11a] and FAN-42[11b] in 2011 and 2013, respectively). Subsequently, Hoberg's group and Mateo-Alonso's group synthesized FAN-54[12] and FAN-90[13] with even larger pore sizes in 2018 and 2022. Meanwhile, Feng's group obtained pyrazine-linked MPc-pz-COF by reacting compound **2** with an porphyrin aromatic amine.[14] Generally speaking, compounds **1**−**3** mainly formed linear or star-shaped PAHs and N-PAHs as well as two-dimensional COF materials.

To further develop N-PAHs with different shapes, compound **4** was developed in 1997, and Bunz's group used this building block to synthesize a series of Z-shaped N-heterophenes and investigated their properties as OLED materials.[15] Recently, Alonso's group utilized TIPS-functionalized compound **4** (TIPS = bis-triisopropylsilylethynyl) to obtain planar and helical dinaphthophenazines.[16] Meanwhile, Zhang's group synthesized the isomer **5** of compound **4** and a series of its U-shaped helical azaarene derivatives.[17] Aside from these planar polyketone building blocks, many other new polyketone building blocks were also developed, such as dibenzoanthradiquinone,[18] homosumanene orthoquinone,[19] etc. Our group also reported the preparation of a series of fused heteroaromatic diones through double intramolecular Friedel−Crafts acylation, and it is worth mentioning that the dione product transformed from difuran, dipyrryole, and dibenzofuran substrates were first reported in that work.[20]

For the organic functional materials derived from planar polyketone building blocks, they are generally also planar, and it is necessary to develop non-planar or twisted or three-dimensional polyketone building blocks to further enlarge the types of organic functional materials and explore their potential

Received: June 22, 2023
Accepted: August 15, 2023
Published: August 25, 2023

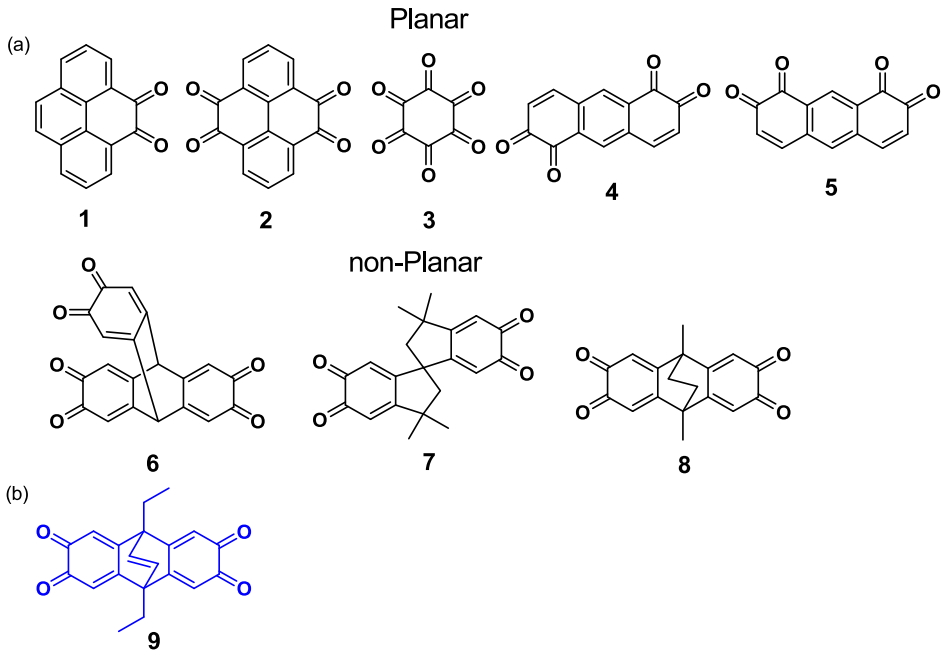

Figure 1. (a) Selective structures of ketone compounds reported in the literature; (b) polyketone building block in this work.

properties. Toward this aim, Wuest's group used 2,3-dichloro-5,6-dicyano1,4-benzoquinone (DDQ) as the oxidation reagent to synthesize triptycene triquinone **6**,[21] which can be used as a cathode material itself for higher-energy alkali metal batteries,[22] and it can be converted into phenazine derivatives subsequently.[23] In addition, triptycene-based microporous poly(benzimidazole) networks can be synthesized from 9,10-dimethyl-substituted **6**.[24] Bunz's group synthesized the spiroketone compound **7** and used its azaacene dimers as organic photovoltaic acceptor materials, affording a maximum power conversion efficiency up to 1.6%.[25] Recently, Bunz's group also synthesized **8** and further converted it into dimeric phenazinothiadiazole and applied them as acceptors in bulk heterojunction solar cells.[26]

From the above elaboration, despite that various polyketone building blocks have been developed, regardless of whether they are planar or non-planar ones, one issue is that there are only carbonyl groups on the molecular skeleton, which will constrain their transformation to some extent (e.g., at present, mostly focusing on the condensation reaction between amine and ketone reactants) and further limit the development of new functional materials. Hence, it is still a challengeable work to introduce additional functional groups on the existing polyketone molecular skeleton to enlarge the types of reaction as far as possible. As we know, vinyl is a fairly fundamental functional group that can undergo the oxidation reaction (conversion into the diol group), polymerization reaction, ring-opening reaction, etc. Hence, we are interested in whether it is possible to combine vinyl and polyketone functional groups together into one molecule. In this work, we reported the design and synthesis of the building block 9,10-diethyl-9,10-ethenoanthracene-2,3,6,7(9*H*,10*H*)-tetraone **9** with additional vinyl functional groups. In addition, N-PAH derivatives (Figure 2) based on compound **9** were also synthesized, and their preliminary photoelectrical properties were studied.

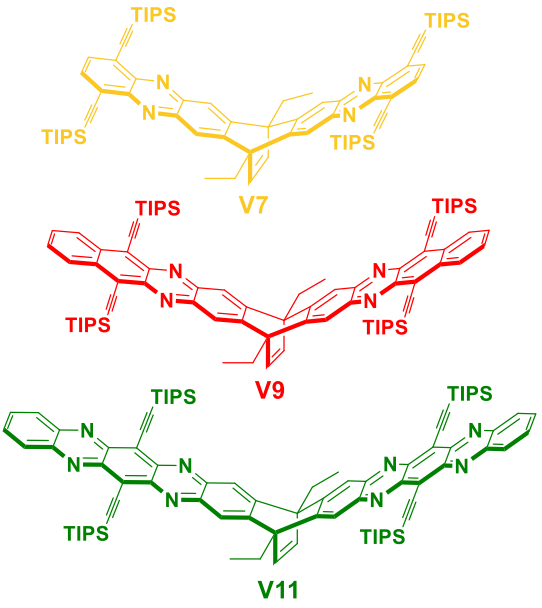

Figure 2. Chemical structures of **V7**, **V9**, and **V11**.

RESULTS AND DISCUSSION

Synthesis. Scheme 1 shows the synthetic route of compound **9**. A solution of veratrole and propanal was added dropwise into 84% sulfuric acid to obtain **10**.[27] The key to this reaction is to control the low temperature of the reaction and the slow rate of dropwise addition of the mixed solution. In addition, during post-processing, we added ammonia dropwise to the reaction solution according to the reported literature[27] and then filtered the reaction mixture, obtaining only a black solid. Then, we changed the method by pouring the reaction solution directly into 300 mL ice-methanol, then filtered, and washed repeatedly with methanol to obtain the off-white solid product **10** in a relatively high yield of 67%. Compound **10** and dimethyl acetylenedicarboxylate underwent the Diels–Alder addition reaction to obtain

https://doi.org/10.1021/acsomega.3c04452
ACS Omega 2023, 8, 32931−32939

Scheme 1. Synthetic Route of 9

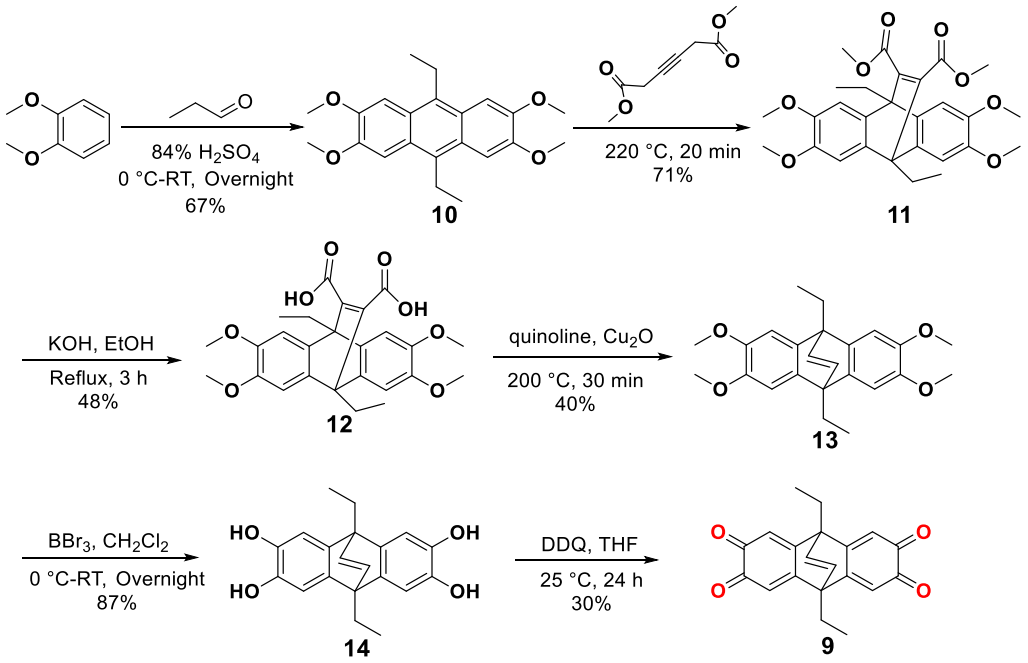

Scheme 2. Synthesis of V-Shaped Azaacenes V7, V9, and V11

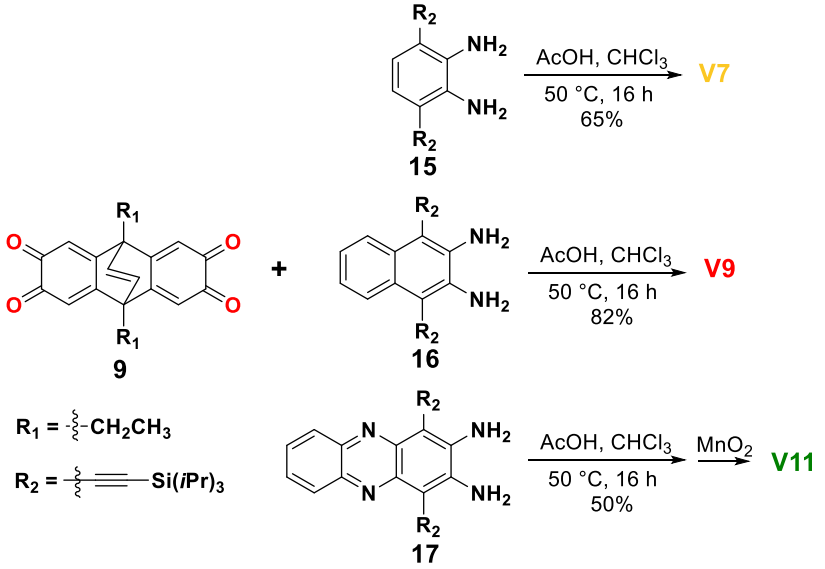

11. After the hydrolysis reaction of **11**, the two ester groups changed into two carboxyl groups to afford the pale yellow solid **12**. We put **12** into the reaction tube, added CuO and quinoline, and carried out the decarboxylation reaction at 240 °C,[28a,b] but the product was not obtained. Then, we adjusted the temperature in the range of 200−280 °C but still failed. Finally, under the guidance of literature,[28c] we replaced copper oxide with Cu_2O and maintained the reaction at 200 °C for 30 min, and finally obtained a beige solid product **13** by column chromatography. The four methoxyl groups of **13** were removed using boron tribromide [(1 M in dichloromethane (DCM)].[21] It is important to note that the temperature must be kept below 0 °C, and the boron tribromide solution cannot be added too fast. During the post-processing, we initially extracted with ethyl acetate and then concentrated by evaporation, only resulting in a dark black solid with a lower purity of the desired product. Later, we poured the reaction system into ice water and then allowed it to stand in the fume hood about 10 min. After that, we filtered it directly and washed the solid with petroleum ether, obtaining the light purple solid product **14** with higher purity. Finally, the hydroxyl groups were oxidized to carbonyl groups in the presence of the oxidant DDQ[29] to obtain **9**. The residue was chromatographed on silica gel (petroleum ether/ethyl acetate = 2:1) and dried under vacuum to afford a dark green solid, which is stable in the solid state. Their structures were confirmed by ^{1}H NMR, ^{13}C NMR, and MS, as shown in Figures S1−8 and S21−22 in the Supporting Information.

Scheme 2 shows the synthetic route of novel V-shaped azaacenes. The 2-fold condensation reactions between tetraone **9** and diamines **15**,[30] **16**,[31] and **17**[32] gave the azaacene dimers in moderate to good yields. We initially chose the reaction

https://doi.org/10.1021/acsomega.3c04452
ACS Omega 2023, 8, 32931−32939

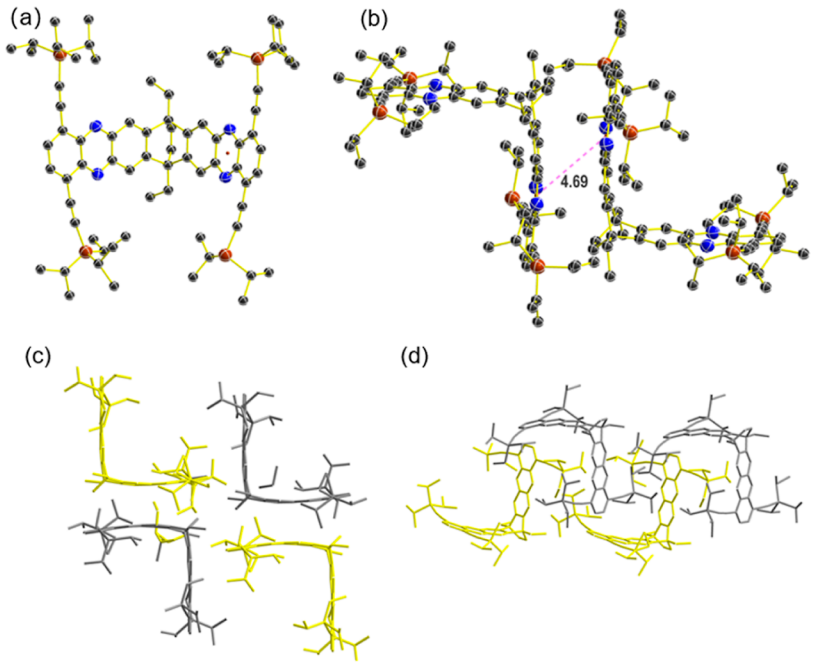

Figure 3. Illustration of the X-ray crystal structure of **V7**: (a) structure of **V7** in the solid state; (b) back-to-back feature between two V-shaped structures [indicated by pink dashed lines, numbers refer to distances (Å)]; (c,d) different projections of part of the **V7** packing mode.

Scheme 3. Synthesis of Reported Azaacenes N3, N4, and N5

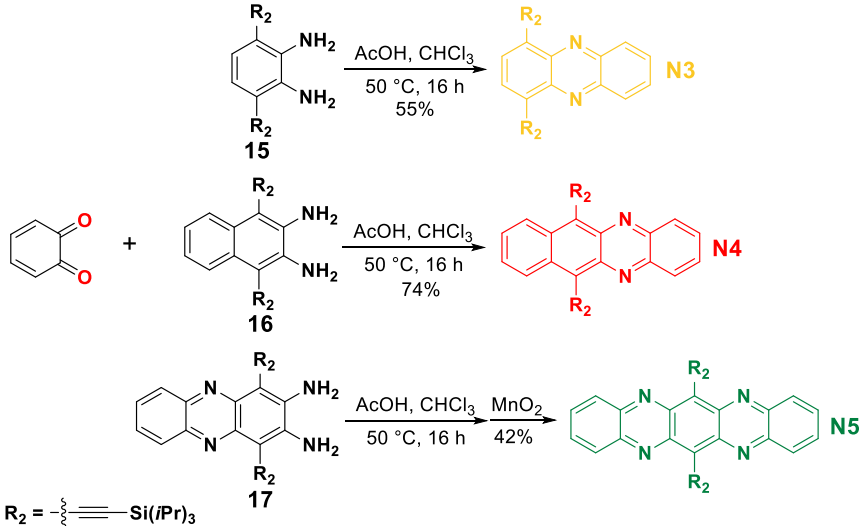

temperature at 100 °C but obtained a very low yield of the product. Then, we gradually lowered the reaction temperature and obtained a much increased yield at 50 °C. The tetraone compound is unstable in the solution state, and a too high temperature will accelerate its deterioration, so an appropriate lower temperature is beneficial to the reaction. It should be noted that compared to **V7** and **V9**, synthesis of **V11** requires the addition of manganese dioxide. Their structures were confirmed by ^{1}H NMR, ^{13}C NMR, and MS, as shown in Figures S9−14 and S23−25 in the Supporting Information.

Single crystals of V-shaped azaacenes were grown by the volatilization of methanol into chlorobenzene or chloroform. Unfortunately, we just got the single crystal of **V7** which was suitable for X-ray diffraction analysis. **V7** crystallized in triclinic symmetry with the association of *P*-1 space group, as shown in Figure 3a, and the crystal data and structure refinement information of **V7** are summarized in Table S1. With one unit cell containing two independent V-shaped structures, the lattice features back-to-back stacking with a distance of 4.69 Å (Figure 3b, distance between centroids of the azaacene rings). Notably, the occupation of each sterically hindered triisopropylsilyl group in funnel-like cavity also influenced the layer stacking pattern, indicating the stacked structure hand-in-hand visually (Figure 3c,d).

Scheme 3 shows the synthetic route of reported azaacenes **N3**,[33] **N4**,[34] and **N5**.[35] Unlike the previously reported literature, we lowered the reaction temperature this time because 1,2-benzoquinone was unstable, so lowering the reaction temperature helped to increase the productivity. It is worth mentioning that in previous reports,[36] the condensation of 1,2-benzoquinone and diamine **17** could not give compound **N5**, but we successfully realized this reaction. It should be

https://doi.org/10.1021/acsomega.3c04452
ACS Omega 2023, 8, 32931−32939

noted that after the completion of the reaction of 1,2-benzoquinone and diamine **17**, it is necessary to add manganese dioxide to obtain the final product **N5**. Their structures were confirmed by ^{1}H NMR and ^{13}C NMR, as shown in Figures S15−20 in the Supporting Information.

Optical Properties. Figure 4 shows the UV−vis absorption spectra of azaacenes. There are distinct increases in λ_{max} (Table 1) from **N3** to **N5** and from **V7** to **V11**, which indicates the absorption bathochromic shift with the increase of conjugation length. V-shaped azaacenes can be viewed as symmetric dimer structures and exhibited almost same values of λ_{max} and λ_{onset} compared to their corresponding monomer molecules (Figure S26), which indicates that the central 9,10-functional carbon has no influence on their optical properties. However, the UV absorption intensity of V-shaped molecules is all stronger than that of monomer molecules through 300−800 nm, which can be attributed to the 2-fold azaacene backbone in the V-shaped molecules.

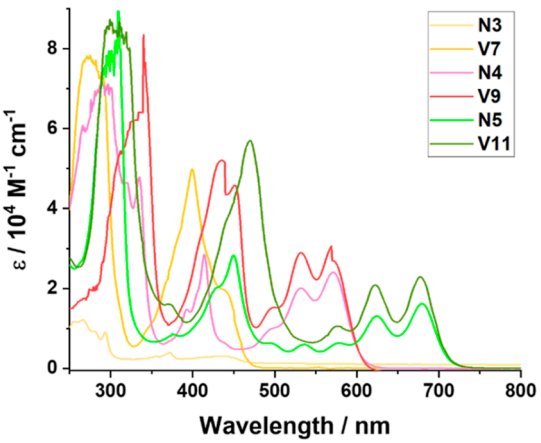

Figure 4. UV−vis absorption spectra of azaacenes in DCM (4×10^{-5} M).

Table 1. Optical and Electronic Properties of V7, V9, and V11

compd	λ_{max} (nm)	λ_{onset} (nm)	EMS$_{max}$ (nm)	LUMO (eV) mes[a] /cal[b]	HOMO (eV) mes[c] /cal[b]	gap (eV) mes[d]/cal[b]
V7	441	471	496	−3.57/−2.91	−6.20/−5.80	2.63/2.90
V9	569	612	613	−3.66/−3.18	−5.69/−5.36	2.03/2.18
V11	681	725	705	−4.04/−3.67	−5.77/−5.46	1.73/1.79
N3	440	471	492	−3.72/−3.06	−6.35/−6.03	2.63/2.97
N4	569	612	615	−3.73/−3.50	−5.76/−5.54	2.03/2.04
N5	681	725	713	−4.07/−3.43	−5.80/−5.29	1.73/1.86

[a] $E_{LUMO}^{mes} = -[4.8 - E_{Fc} + E_{re}^{onset}]$ (eV). [b] DFT calculations (B3LYP/6-31G*) using Gaussian09. [c] $E_{HOMO} = E_{LUMO} - E_{gap(opt)}$ (eV). [d] Optical band gaps were calculated from 1240 nm/λ_{onset}.

Figures 5 and S27 show the fluorescence diagrams of V-shaped azaacenes and their corresponding monomers that clearly highlight the red shift and differences of fluorescence intensity (Table 1). It is distinct that the fluorescence intensity of **V7** is stronger than that of **N3**, and the intensity of **V9** is slightly greater than that of **N4**. The fluorescence intensity of **N4** and **V9** is strongest among all the molecules. Nevertheless, the fluorescence intensity of **V11** is much less than that of **N5**. The quantum yields for **V7**, **V9**, and **V11** were measured to be 3.08, 12.37, and 1.20%, respectively (Figure S28). From the previous UV−vis diagram, the UV absorption intensity of **V11** is greater than that of **N5**, indicating that the dimer azaacene **V11** undergoes some special process during relaxation from the excited state to the ground state, which leads to fluorescence quenching, and we are currently studying this phenomenon.

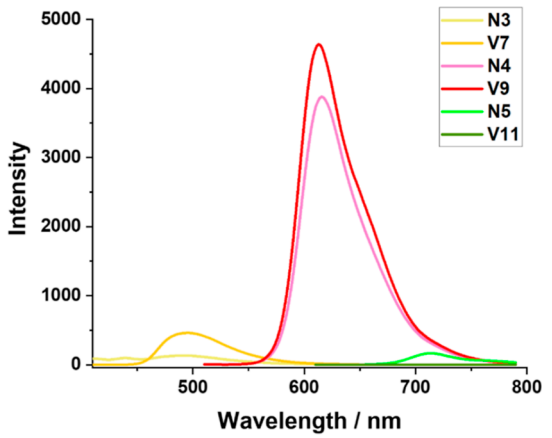

Figure 5. Emission spectra of azaacenes in DCM (4×10^{-5} M) (excitation wavelength: 410 nm for **N3** and **V7**, 510 nm for **N4** and **V9**, and 610 nm for **N5** and **V11**).

Electrochemistry and Quantum Chemical Calculations. Cyclic voltammograms of V-shaped azaacenes were performed in DCM at room temperature (Figure 6). Due to the presence of triisopropylsilyl and ethyl groups, V-shaped azaacenes are well soluble in DCM. The measured E_{re}^{onset} values of **V7**, **V9**, and **V11** were −0.76, −0.66, and −0.29 V, respectively. V-shaped molecules and monomer molecules have similar values of LUMO energy levels, and the values change in the same trend as the conjugation length of the molecule increases (Table 1 and Figure S29). The experimentally measured LUMOs of V-shaped azaacenes are

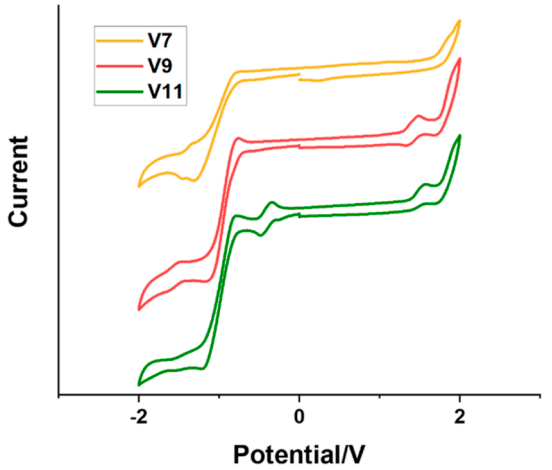

Figure 6. Cyclic voltammograms of **V7**−**V11** in 0.1 M *n*-Bu$_4$NPF$_6$ solution of DCM at a scan rate of 100 mV s^{-1}.

https://doi.org/10.1021/acsomega.3c04452
ACS Omega 2023, 8, 32931−32939

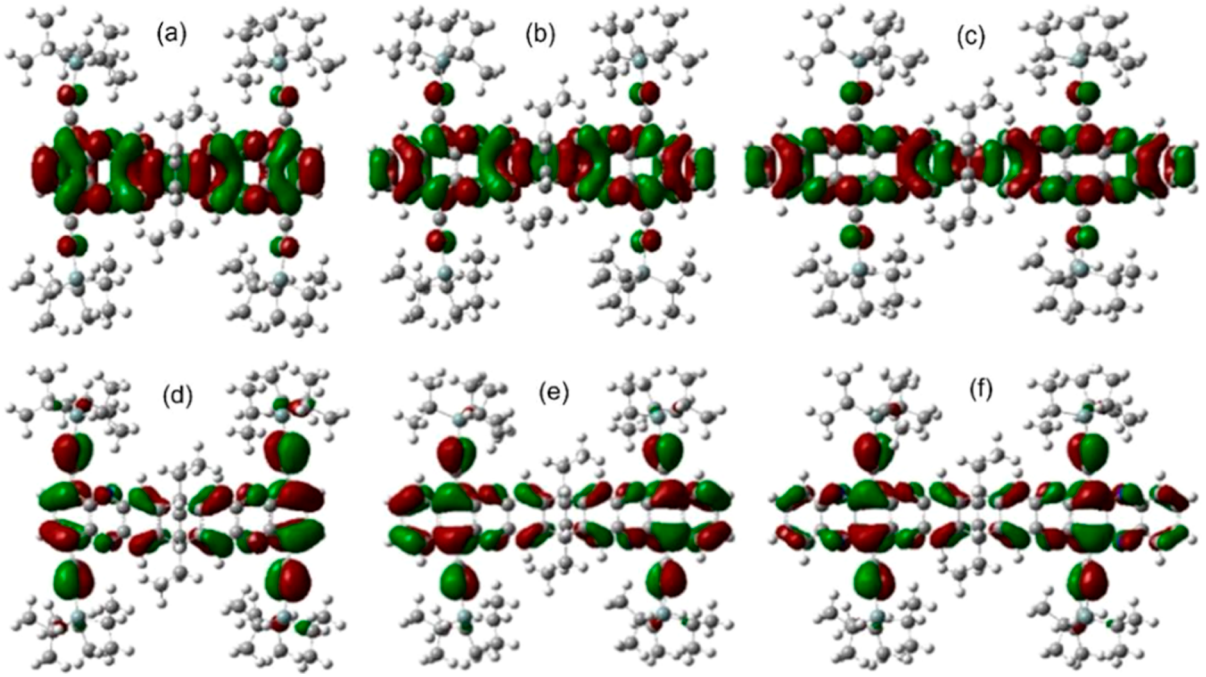

Figure 7. Quantum-chemical calculations of the FMOs (LUMOs, top; HOMOs, bottom): (a,d) **V7**; (b,e) **V9**; (c,f) **V11**.

deeper than those of S-shaped and U-shaped isomers (Figures S30 and 31, Table S2). This can be attributed to their symmetrical structures, which allows V-shaped azaacenes with the same benzenoid ring number to have a longer conjugation length than S-shaped and U-shaped isomers.

The B3LYP density functional method with the D3(BJ) dispersion was used. The correction was employed in this work to carry out all the computations. The 6-31G(d) basis set was used for the atoms in geometry optimizations using the polarizable continuum model with DCM as the solvent. All DFT theoretical calculations were carried out using the Gaussian09 program package[37] (Figure 7). It is obvious that the frontier molecular orbitals (FMOs) of V-shaped azaacenes are similar to their corresponding monomer molecules. From the MO diagrams, the LUMOs of V-shaped azaacenes are delocalized over the molecular backbone. The HOMOs are distributed in their linear fused ring sections. The trends of theoretical calculations of the LUMO/HOMO of **V7**, **V9**, and **V11** are consistent with the experimentally measured trends. All the data are summarized in Table 1.

CONCLUSIONS

In summary, we have designed and synthesized a tetraketone building block that reacted with different diamine compounds to obtain a series of symmetric V-shape azaacenes. Solid structure of **V7** was clearly revealed by the single-crystal X-ray analysis. The optical and electronic properties of V-shaped azaacenes were measured and compared with their corresponding monomer molecules and their S-shaped and U-shaped analogues. Both the synthesized tetraone compound and V-shaped azaacenes have vinyl double bonds, which can be used as reaction sites to obtain other new organic functional materials.

EXPERIMENTAL SECTION

Synthesis of Tetraone 9. *Compounds 10−12.* Compounds **10−12** were synthesized according to the methods reported in the literature[27] (see detailed synthesis process section in the Supporting Information). The reaction mixture of veratrole and propanal added dropwise into 80% concentrated sulfuric acid gave **10**, which can be reacted with dimethyl butynedioate at 220 °C to give **11**. Compound **11** underwent a hydrolysis reaction in the environment of potassium hydroxide to give **12**.

Compound 13. Compound **12** (1.00 g, 2.13 mmol) and Cu_2O (0.31 g, 2.13 mmol) were added into quinoline (5 mL). The resulting mixture was heated at 200 °C under a nitrogen atmosphere for 30 min. After cooling, the filtrate was acidified with 4 N HCl (20 mL). The mixture was extracted with DCM. The organic layer was dried and evaporated under reduced pressure. The residue was chromatographed on silica gel (eluent: DCM) to give a white solid in 40% yield. ^{1}H NMR (600 MHz, chloroform-*d*): δ 6.96 (s, 2H), 6.88 (s, 4H), 3.85 (s, 12H), 2.66 (q, J = 7.4 Hz, 4H), 1.50 (t, J = 7.4 Hz, 6H). ^{13}C{^{1}H} NMR (151 MHz, chloroform-*d*): δ 144.9, 143.3, 141.8, 106.6, 56.4, 52.9, 21.4, 9.9. HRMS (ESI) m/z: $[M + H]^+$ calcd for $C_{24}H_{28}O_4$, 381.2021; found, 381.2055.

Compound 14. Compound **13** (1.00 g, 2.63 mmol) was dissolved in DCM (20 mL), and the resulting solution was cooled to below 0 °C and kept at this temperature under a N_2 atmosphere. A solution of BBr_3 (1 M in DCM, 2.63 mL) was then added dropwise to the reaction mixture over a period of 30 min. After complete addition, the reaction temperature was gradually allowed to reach room temperature, and the stirring was continued for 6 h. After the reaction was completed, the reaction mixture was poured into ice water and then filtered to obtain a light purple solid in 87% yield. ^{1}H NMR (600 MHz, DMSO-d_6): δ 6.77 (s, 2H), 6.57 (s, 4H), 2.35 (q, J = 7.4 Hz, 4H), 1.31 (t, J = 7.4 Hz, 6H).

Compound 9. DDQ (1.55 g, 6.83 mmol) was added to a suspension of **14** (0.20 g, 0.63 mmol) in anhydrous oxygen-free THF (10 mL) under an atmosphere of N_2. The mixture was stirred at 25 °C for 24 h, and the resulting suspension was evaporated under reduced pressure. The residue was dissolved

https://doi.org/10.1021/acsomega.3c04452
ACS Omega 2023, 8, 32931−32939

in DCM, then the mixture was filtered, and the filtrate was dried and evaporated under reduced pressure. The residue was chromatographed on silica gel (petroleum ether/ethyl acetate = 2:1) and dried under vacuum to afford a dark green solid in 30% yield. ^{1}H NMR (600 MHz, DMSO-d_6): δ 6.57 (s, 2H), 6.22 (s, 4H), 2.15 (s, 4H), 1.15 (s, 6H). ^{13}C{^{1}H} NMR (151 MHz, DMSO-d_6): δ 179.5, 153.1, 134.0, 121.6, 49.9, 20.3, 9.07. HRMS (ESI) m/z: [M + H]$^+$ calcd for $C_{20}H_{16}O_4$, 323.1082; found, 323.1274.

Synthesis of Azaacenes V7, V9, and V11. *Compound V7*. Tetraone **9** (30 mg, 0.094 mmol) and diamine **15** (103.03 mg, 0.22 mmol) were added to a solvent mixture of chloroform (1 mL) and acetic acid (1 mL) in a round-bottom flask equipped with a condenser. The mixture was stirred at 50 °C for 16 h. After cooling to room temperature, the solvent was removed under reduced pressure. The crude product was purified by column chromatography on silica gel using the solvent mixture (hexane/DCM = 5:1) to obtain the red product in 65% yield. ^{1}H NMR (600 MHz, chloroform-d): δ 8.04 (s, 4H), 7.89 (s, 4H), 6.99 (s, 2H), 3.02 (q, J = 7.4 Hz, 4H), 1.68 (t, J = 7.3 Hz, 6H), 1.31−1.28 (m, 84H). ^{13}C{^{1}H} NMR (151 MHz, chloroform-d): δ 149.2, 143.3, 142.5, 138.6, 133.0, 124.2, 121.2, 103.8, 100.5, 52.2, 21.3, 18.9, 11.6, 9.5. HRMS (APCI) m/z: [M + H]$^+$ calcd for $C_{76}H_{104}N_4Si_4$, 1185.7372; found, 1185.7428.

Compound V9. Tetraone **9** (30 mg, 0.094 mmol) and diamine **16** (115.66 mg, 0.22 mmol) were added to a solvent mixture of chloroform (1.5 mL) and acetic acid (1.5 mL) in a round-bottom flask equipped with a condenser. The mixture was stirred at 50 °C for 16 h. After cooling to room temperature, the solvent was removed under reduced pressure. The crude product was purified by column chromatography on silica gel using the solvent mixture (hexane/DCM = 4:1) to obtain the red product in 82% yield. ^{1}H NMR (600 MHz, chloroform-d): δ 8.73−8.63 (m, 4H), 8.02 (d, J = 9.9 Hz, 4H), 7.63 (tt, J = 5.8, 2.5 Hz, 4H), 6.97 (d, J = 1.8 Hz, 2H), 3.02 (q, J = 7.4 Hz, 4H), 1.70 (t, J = 7.3 Hz, 6H), 1.41−1.33 (m, 84H). ^{13}C{^{1}H} NMR (151 MHz, chloroform-d): δ148.9, 143.7, 141.3, 138.1, 134.7, 127.6, 121.3, 120.6, 107.7, 103.0, 51.9, 29.7, 21.3, 19.0, 11.7, 9.5. HRMS (APCI) m/z: [M + H]$^+$ calcd for $C_{84}H_{104}N_4Si_4$, 1285.7685; found, 1285.7675.

Compound V11. Tetraone **9** (30 mg, 0.094 mmol) and diamine **17** (125.48 mg, 0.22 mmol) were added to a solvent mixture of chloroform (1.5 mL) and acetic acid (1.5 mL) in a round-bottom flask equipped with a condenser. The mixture was stirred at 50 °C for 16 h. After cooling to room temperature, the solvent was partially removed under reduced pressure. MnO_2 was added into the solution, and the mixture was stirred at room temperature for 12 h. Then, the mixture was filtered, and the filtrate was dried and evaporated under reduced pressure. The crude product was purified by column chromatography on silica gel using the solvent mixture (hexane/DCM = 1:1) to obtain the dark green product in 50% yield. ^{1}H NMR (600 MHz, chloroform-d): δ 8.24 (dd, J = 6.9, 3.4 Hz, 4H), 8.04 (s, 4H), 7.87−7.80 (m, 4H), 6.98 (s, 2H), 3.05 (d, J = 7.5 Hz, 4H), 1.73 (t, J = 7.4 Hz, 6H), 1.47−1.38 (m, 84H). ^{13}C{^{1}H} NMR (151 MHz, chloroform-d): δ 149.6, 145.3, 144.8, 143.0, 142.6, 137.8, 131.9, 130.6, 122.6, 121.6, 112.0, 103.1, 51.9, 21.4, 19.0, 11.8, 9.4. HRMS (ESI) m/z: [M + H]$^+$ calcd for $C_{88}H_{108}N_8Si_4$, 1389.7808; found, 1389.7899.

■ ASSOCIATED CONTENT

Supporting Information

The Supporting Information is available free of charge at https://pubs.acs.org/doi/10.1021/acsomega.3c04452.

General information on materials and methods, detailed synthesis process for compounds **10**−**12** and **N3**−**N5**, ^{1}H NMR spectra for all compounds, ^{13}C NMR spectra for compounds **9**, **13**, **V7**, **V9**, **V11**, and **N3**−**N5**, MS spectra for compounds **9**, **13**,**V7**, **V9**, and **V11**, UV−vis spectra, emission spectra, quantum yield results, cyclic voltammetry curves for ferrocene, structures of S-shaped and U-shaped azaarenes, optical and electronic data of S-shaped and U-shaped azaarenes, and crystal data and structure refinement for **V7** (PDF)

CIF data for **V7** (CIF)

■ AUTHOR INFORMATION

Corresponding Authors

Wangqiao Chen − *Guangdong Provincial Key Laboratory of Optical Information Materials and Technology & Institute of Electronic Paper Displays, South China Academy of Advanced Optoelectronics, South China Normal University, Guangzhou 510631, China*; orcid.org/0000-0002-1551-8422; Email: wqchen@m.scnu.edu.cn

Guofu Zhou − *Guangdong Provincial Key Laboratory of Optical Information Materials and Technology & Institute of Electronic Paper Displays, South China Academy of Advanced Optoelectronics, South China Normal University, Guangzhou 510631, China*; orcid.org/0000-0003-1101-1947; Email: guofu.zhou@m.scnu.edu.cn

Authors

Hong Chen − *Guangdong Provincial Key Laboratory of Optical Information Materials and Technology & Institute of Electronic Paper Displays, South China Academy of Advanced Optoelectronics, South China Normal University, Guangzhou 510631, China*

Shilong Zhang − *Guangdong Provincial Key Laboratory of Optical Information Materials and Technology & Institute of Electronic Paper Displays, South China Academy of Advanced Optoelectronics, South China Normal University, Guangzhou 510631, China*

Jinlei Liu − *Guangdong Provincial Key Laboratory of Optical Information Materials and Technology & Institute of Electronic Paper Displays, South China Academy of Advanced Optoelectronics, South China Normal University, Guangzhou 510631, China*

Jiaxin Li − *Guangdong Provincial Key Laboratory of Optical Information Materials and Technology & Institute of Electronic Paper Displays, South China Academy of Advanced Optoelectronics, South China Normal University, Guangzhou 510631, China*

Complete contact information is available at: https://pubs.acs.org/10.1021/acsomega.3c04452

Notes

The authors declare no competing financial interest.

■ ACKNOWLEDGMENTS

The present research was financially sponsored by National Key R&D Program of China (2021YFB3600601) and Science and Technology Program of Guangzhou (nos. 202201010103

and 2019050001), National Natural Science Foundation of China (no. 21905100), Program for Guangdong Innovative and Entrepreneurial Teams (no. 2019BT02C241), and Guangdong Provincial Key Laboratory of Optical Information Materials and Technology (no. 2017B030301007).

REFERENCES

(1) (a) Watanabe, M.; Chen, K. Y.; Chang, Y. J.; Chow, T. J. Acenes Generated from Precursors and Their Semiconducting Properties. *Acc. Chem. Res.* **2013**, *46*, 1606−1615. (b) Ye, Q.; Chi, C. Recent Highlights and Perspectives on Acene Based Molecules and Materials. *Chem. Mater.* **2014**, *26*, 4046−4056. (c) Li, J.; Chen, S.; Wang, Z.; Zhang, Q. Pyrene-fused Acenes and Azaacenes: Synthesis and Applications. *Chem. Rec.* **2016**, *16*, 1518−1530. (d) Mateo-Alonso, A. Synthetic Approaches to Pyrene-Fused Twistacenes. *Eur. J. Org Chem.* **2017**, 7006−7011. (e) Müller, M.; Ahrens, L.; Brosius, V.; Freudenberg, J.; Bunz, U. H. F. Unusual Stabilization of Larger Acenes and Heteroacenes. *J. Mater. Chem. C* **2019**, *7*, 14011−14034. (f) Chen, W.; Yu, F.; Xu, Q.; Zhou, G.; Zhang, Q. Recent Progress in High Linearly Fused Polycyclic Conjugated Hydrocarbons (PCHs, n > 6) with Well-Defined Structures. *Adv. Sci.* **2020**, *7*, 1903766.

(2) (a) Mateo-Alonso, A. Pyrene-fused pyrazaacenes: from small molecules to nanoribbons. *Chem. Soc. Rev.* **2014**, *43*, 6311−6324. (b) Bunz, U. H. F.; Freudenberg, J. N-Heteroacenes and N-Heteroarenes as N-Nanocarbon Segments. *Acc. Chem. Res.* **2019**, *52*, 1575−1587. (c) Said, A. A.; Xie, J.; Zhang, Q. Recent Progress in Organic Electron Transport Materials in Inverted Perovskite Solar Cells. *Small* **2019**, *15*, No. e1900854. (d) Zhang, Z.; Zhang, Q. Recent Progress in Well-defined Higher Azaacenes (n ≥ 6): Synthesis, Molecular Packing, and Applications. *Mater. Chem. Front.* **2020**, *4*, 3419−3432. (e) Ahrens, L.; Rominger, F.; Freudenberg, J.; Bunz, U. H. F. Etheno-bridged Azaacene Spiro Dimers. *Chem.—Eur. J.* **2023**, *29*, No. e202301018. (f) Li, G.; Wu, Y.; Gao, J.; Li, J.; Zhao, Y.; Zhang, Q. Synthesis, Physical Properties, and Anion Recognition of Two Novel Larger Azaacenes: Benzannelated Hexazaheptacene and Benzannelated N,N′-Dihydrohexazaheptacene. *Chem.—Asian J.* **2013**, *8*, 1574−1578. (g) Zhang, Z.; Wang, Z.; Aratani, N.; Zhu, X.; Zhang, Q. Seeing Is Believing: A Wavy N-Heteroarene with 20 Six-Membered Rings Linearly Annulated in a Row. *CCS Chem.* **2022**, *4*, 3491−3496. (h) Li, G.; Duong, H. M.; Zhang, Z.; Xiao, J.; Liu, L.; Zhao, Y.; Zhang, H.; Huo, F.; Li, S.; Ma, J.; Wudl, F.; Zhang, Q. Approaching a stable, green twisted heteroacene through "clean reaction" strategy. *Chem. Commun.* **2012**, *48*, 5974−5976. (i) Wang, Z.; Gu, P.; Liu, G.; Yao, H.; Wu, Y.; Li, Y.; Rakesh, G.; Zhu, J.; Fu, H.; Zhang, Q. A large pyrene-fused N-heteroacene: fifteen aromatic six-membered rings annulated in one row. *Chem. Commun.* **2017**, *53*, 7772−7775.

(3) (a) Geng, K.; He, T.; Liu, R.; Dalapati, S.; Tan, K. T.; Li, Z.; Tao, S.; Gong, Y.; Jiang, Q.; Jiang, D. Covalent Organic Frameworks: Design, Synthesis, and Functions. *Chem. Rev.* **2020**, *120*, 8814−8933. (b) Cusin, L.; Peng, H.; Ciesielski, A.; Samorì, P. Chemical Conversion and Locking of the Imine Linkage: Enhancing the Functionality of Covalent Organic Frameworks. *Angew. Chem., Int. Ed.* **2021**, *60*, 14236−14250. (c) Guo, F.; Zhang, W.; Yang, S.; Wang, L.; Yu, G. 2D Covalent Organic Frameworks Based on Heteroacene Units. *Small* **2023**, *19*, No. e2207876. (d) Guan, Q.; Zhou, L.-L.; Dong, Y.-B. Construction of Covalent Organic Frameworks via Multicomponent Reactions. *J. Am. Chem. Soc.* **2023**, *145*, 1475−1496. (e) Meng, Z.; Aykanat, A.; Mirica, K. A. Proton Conduction in 2D Aza-Fused Covalent Organic Frameworks. *Chem. Mater.* **2019**, *31*, 819−825. (f) Wang, P.-L.; Ding, S.-Y.; Zhang, Z.-C.; Wang, Z.-P.; Wang, W. Constructing Robust Covalent Organic Frameworks via Multicomponent Reactions. *J. Am. Chem. Soc.* **2019**, *141*, 18004−18008. (g) Tian, Z.; Kale, V. S.; Wang, Y.; Kandambeth, S.; Czaban-Jóźwiak, J.; Shekhah, O.; Eddaoudi, M.; Alshareef, H. N. High-Capacity $NH4^+$ Charge Storage in Covalent Organic Frameworks. *J. Am. Chem. Soc.* **2021**, *143*, 19178−19186.

(4) Hu, J.; Zhang, D.; Harris, F. W. Ruthenium(III) Chloride Catalyzed Oxidation of Pyrene and 2,7-Disubstitued Pyrenes: An Efficient, One-Step Synthesis of Pyrene-4,5-diones and Pyrene-4,5,9,10-tetraones. *J. Org. Chem.* **2005**, *70*, 707−708.

(5) Xiao, J.; Duong, H. M.; Liu, Y.; Shi, W.; Ji, L.; Li, G.; Li, S.; Liu, X. W.; Ma, J.; Wudl, F.; Zhang, Q. Synthesis and Structure Characterization of a Stable Nonatwistacene. *Angew. Chem., Int. Ed.* **2012**, *51*, 6094−6098.

(6) Chen, W.; Li, X.; Long, G.; Li, Y.; Ganguly, R.; Zhang, M.; Aratani, N.; Yamada, H.; Liu, M.; Zhang, Q. Pyrene-Containing Twistarene: Twelve Benzene Rings Fused in a Row. *Angew. Chem., Int. Ed.* **2018**, *57*, 13555−13559.

(7) Gu, P.-Y.; Wang, Z.; Liu, G.; Yao, H.; Wang, Z.; Li, Y.; Zhu, J.; Li, S.; Zhang, Q. Synthesis, Full Characterization, and Field Effect Transistor Behavior of a Stable Pyrene-Fused N-Heteroacene with Twelve Linearly Annulated Six-Membered Rings. *Chem. Mater.* **2017**, *29*, 4172−4175.

(8) Kohl, B.; Rominger, F.; Mastalerz, M. A Pyrene-fused N-heteroacene with Eleven Rectilinearly Annulated Aromatic Rings. *Angew. Chem., Int. Ed.* **2015**, *54*, 6051−6056.

(9) Hu, B.-L.; Zhang, K.; An, C.; Schollmeyer, D.; Pisula, W.; Baumgarten, M. Layered Thiadiazoloquinoxaline-Containing Long Pyrene-Fused N-Heteroacenes. *Angew. Chem., Int. Ed.* **2018**, *57*, 12375−12379.

(10) Dubey, R. K.; Melle-Franco, M.; Mateo-Alonso, A. Twisted Molecular Nanoribbons with up to 53 Linearly-Fused Rings. *J. Am. Chem. Soc.* **2021**, *143*, 6593−6600.

(11) (a) Kou, Y.; Xu, Y.; Guo, Z.; Jiang, D. Supercapacitive Energy Storage and Electric Power Supply Using an Aza-fused pi-Conjugated Microporous Framework. *Angew. Chem., Int. Ed.* **2011**, *50*, 8753−8757. (b) Guo, J.; Xu, Y.; Jin, S.; Chen, L.; Kaji, T.; Honsho, Y.; Addicoat, M. A.; Kim, J.; Saeki, A.; Ihee, H.; Seki, S.; Irle, S.; Hiramoto, M.; Gao, J.; Jiang, D. Conjugated Organic Framework with Three-dimensionally Ordered Stable Structure and Delocalized pi Clouds. *Nat. Commun.* **2013**, *4*, 2736.

(12) Kuehl, V. A.; Yin, J.; Duong, P. H. H.; Mastorovich, B.; Newell, B.; Li-Oakey, K. D.; Parkinson, B. A.; Hoberg, J. O. A Highly Ordered Nanoporous, Two-Dimensional Covalent Organic Framework with Modifiable Pores, and Its Application in Water Purification and Ion Sieving. *J. Am. Chem. Soc.* **2018**, *140*, 18200−18207.

(13) Riano, A.; Strutynski, K.; Liu, M.; Stoppiello, C. T.; Lerma-Berlanga, B.; Saeki, A.; Marti-Gastaldo, C.; Khlobystov, A. N.; Valenti, G.; Paolucci, F.; Melle-Franco, M.; Mateo-Alonso, A. An Expanded 2D Fused Aromatic Network with 90-Ring Hexagons. *Angew. Chem., Int. Ed.* **2022**, *61*, No. e202113657.

(14) Wang, M.; Ballabio, M.; Wang, M.; Lin, H. H.; Biswal, B. P.; Han, X.; Paasch, S.; Brunner, E.; Liu, P.; Chen, M.; Bonn, M.; Heine, T.; Zhou, S.; Canovas, E.; Dong, R.; Feng, X. Unveiling Electronic Properties in Metal-Phthalocyanine-Based Pyrazine-Linked Conjugated Two-Dimensional Covalent Organic Frameworks. *J. Am. Chem. Soc.* **2019**, *141*, 16810−16816.

(15) Hahn, S.; Koser, S.; Hodecker, M.; Tverskoy, O.; Rominger, F.; Dreuw, A.; Bunz, U. H. F. Alkyne-Substituted N-Heterophenes. *Chem.—Eur. J.* **2017**, *23*, 8148−8151.

(16) Chen, F.; Gu, W.; Saeki, A.; Melle-Franco, M.; Mateo-Alonso, A. A Sterically Congested Nitrogenated Benzodipentaphene with a Double pi-Expanded Helicene Structure. *Org. Lett.* **2020**, *22*, 3706−3711.

(17) Zhao, K.; Long, G.; Liu, W.; Li, D. S.; Gao, W.; Zhang, Q. U-Shaped Helical Azaarenes: Synthesis, Structures, and Properties. *J. Org. Chem.* **2020**, *85*, 291−295.

(18) Martinez, J. I.; Mora-Fuentes, J. P.; Carini, M.; Saeki, A.; Melle-Franco, M.; Mateo-Alonso, A. Dibenzoanthradiquinone Building Blocks for the Synthesis of Nitrogenated Polycyclic Aromatic Hydrocarbons. *Org. Lett.* **2020**, *22*, 4737−4741.

(19) Nishimoto, M.; Uetake, Y.; Yakiyama, Y.; Saeki, A.; Freudenberg, J.; Bunz, U. H. F.; Sakurai, H. Acceleration Effect of Bowl-Shaped Structure in Aerobic Oxidation Reaction: Synthesis of

https://doi.org/10.1021/acsomega.3c04452
ACS Omega 2023, 8, 32931−32939

Homosumanene ortho-Quinone and Azaacene-Fused Homosumanenes. *Chem.—Eur. J.* **2023**, *29*, No. e202203461.
(20) Chen, W.; Tan, S. Y.; Zhao, Y.; Zhang, Q. A Concise Method to Prepare Novel Fused Heteroaromatic Diones through Double Friedel−Crafts Acylation. *Org. Chem. Front.* **2014**, *1*, 391−394.
(21) Langis-Barsetti, S.; Maris, T.; Wuest, J. D. Triptycene 1,2-Quinones and Quinols: Permeable Crystalline Redox-Active Molecular Solids. *J. Org. Chem.* **2018**, *83*, 15426−15437.
(22) Xia, L.; Tang, B.; Wei, J.; Zhou, Z. Recent Advances in Alkali Metal-Ion Hybrid Supercapacitors. *Batteries Supercaps* **2021**, *4*, 1108−1121.
(23) Ushiroguchi, R.; Shuku, Y.; Suizu, R.; Awaga, K. Variable Host−Guest Charge-Transfer Interactions in 1D Channels Formed in a Molecule-Based Honeycomb Lattice of Phenazine Analogue of Triptycene. *Cryst. Growth Des.* **2020**, *20*, 7593−7597.
(24) Zhao, Y.-C.; Cheng, Q.-Y.; Zhou, D.; Wang, T.; Han, B.-H. Preparation and Characterization of Triptycene-based Microporous Poly(benzimidazole) networks. *J. Mater. Chem.* **2012**, *22*, 11509−11514.
(25) Ahrens, L.; Butscher, J.; Brosius, V.; Rominger, F.; Freudenberg, J.; Vaynzof, Y.; Bunz, U. H. F. Azaacene Dimers: Acceptor Materials with a Twist. *Chem.—Eur. J.* **2020**, *26*, 412−418.
(26) Ahrens, L.; Hofstetter, Y. J.; Celik, B.; Butscher, J. F.; Rominger, F.; Freudenberg, J.; Vaynzof, Y.; Bunz, U. H. F. Dimeric Phenazinothiadiazole Acceptors in Bulk Heterojunction Solar Cells. *Org. Mater.* **2021**, *03*, 168−173.
(27) Makhseed, S.; Samuel, J. Microporous Organic Polymers Incorporating Dicarboximide Units for H_2 Storage and Remarkable CO_2 Capture. *J. Mater. Chem. A* **2013**, *1*, 13004−13010.
(28) (a) Hui, C. W.; Mak, T. C. W.; Wong, H. N. C. Synthesis of 1,4,5,16-Tetrahydroxytetraphenylene. *Tetrahedron* **2004**, *60*, 3523−3531. (b) Urgel, J. I.; Hayashi, H.; Di Giovannantonio, M.; Pignedoli, C. A.; Mishra, S.; Deniz, O.; Yamashita, M.; Dienel, T.; Ruffieux, P.; Yamada, H.; Fasel, R. On-Surface Synthesis of Heptacene Organometallic Complexes. *J. Am. Chem. Soc.* **2017**, *139*, 11658−11661. (c) Heinz, W.; Räder, H. J.; Müllen, K. Changing the Size of a Cavity via an Electron-transfer: Synthesis and Reduction of 1,5,22,26-tetraoxa-[5,5]-(2,8)-dibenzo[a,e]cyclooctatetraenophane. *Tetrahedron Lett.* **1989**, *30*, 159−162.
(29) (a) Talapaneni, S. N.; Kim, J.; Je, S. H.; Buyukcakir, O.; Oh, J.; Coskun, A. Bottom-up Synthesis of Fully sp^2 Hybridized Three-dimensional Microporous Graphitic Frameworks as Metal-free Catalysts. *J. Mater. Chem. A* **2017**, *5*, 12080−12085. (b) Yeap, G.-Y.; Abdul Rahim, M.; Lin, C.-M.; Lin, H.-C.; Maeta, N.; Ito, M. M. Synthesis and Liquid Crystalline Studies of Disc-shaped Molecule on Azo-bridged Benzothiazole-phenyl Ethers. *J. Mol. Liq.* **2016**, *223*, 734−740. (c) Nakashima, K.; Shimizu, T.; Kamakura, Y.; Hinokimoto, A.; Kitagawa, Y.; Yoshikawa, H.; Tanaka, D. A New Design Strategy for Redox-active Molecular Assemblies with Crystalline Porous Structures for Lithium-ion Batteries. *Chem. Sci.* **2020**, *11*, 37−43.
(30) Yang, S.; Shan, B.; Xu, X.; Miao, Q. Extension of N-Heteroacenes through a Four-Membered Ring. *Chem.—Eur. J.* **2016**, *22*, 6637−6642.
(31) (a) Tena, A.; Vazquez-Guilló, R.; Marcos-Fernández, A.; Hernández, A.; Mallavia, R. Polymeric Films Based on Blends of 6FDA−6FpDA Polyimide plus Several Copolyfluorenes for CO_2 Separation. *RSC Adv.* **2015**, *5*, 41497−41505. (b) Yen, Y. S.; Ni, J. S.; Hung, W. I.; Hsu, C. Y.; Chou, H. H.; Lin, J. T. Naphtho[2,3-c][1,2,5]thiadiazole and 2H-Naphtho[2,3-d] [1,2,3]triazole-Containing D-A-pi-A Conjugated Organic Dyes for Dye-Sensitized Solar Cells. *ACS Appl. Mater. Interfaces* **2016**, *8*, 6117−6126. (c) Lindner, B. D.; Engelhart, J. U.; Marken, M.; Tverskoy, O.; Appleton, A. L.; Rominger, F.; Hardcastle, K. I.; Enders, M.; Bunz, U. H. Synthesis and Optical Properties of Diaza- and Tetraazatetracenes. *Chem.—Eur. J.* **2012**, *18*, 4627−4633.
(32) Lindner, B. D.; Engelhart, J. U.; Tverskoy, O.; Appleton, A. L.; Rominger, F.; Peters, A.; Himmel, H. J.; Bunz, U. H. F. Stable Hexacenes through Nitrogen Substitution. *Angew. Chem., Int. Ed.* **2011**, *50*, 8588−8591.
(33) (a) Yang, S.; Chu, M.; Miao, Q. Connecting Two Phenazines with a Four-membered Ring: the Synthesis, Properties and Applications of Cyclobuta[1,2-b:3,4-b′]diphenazines. *J. Mater. Chem. C* **2018**, *6*, 3651−3657. (b) Bryant, J. J.; Zhang, Y.; Lindner, B. D.; Davey, E. A.; Appleton, A. L.; Qian, X.; Bunz, U. H. F. Alkynylated Phenazines: Synthesis, Characterization, and Metal-Binding Properties of Their Bis-Triazolyl Cycloadducts. *J. Org. Chem.* **2012**, *77*, 7479−7486.
(34) (a) Miao, S.; Brombosz, S. M.; Schleyer, P. v. R.; Wu, J. I.; Barlow, S.; Marder, S. R.; Hardcastle, K. I.; Bunz, U. H. F. Are N,N-Dihydrodiazatetracene Derivatives Antiaromatic? *J. Am. Chem. Soc.* **2008**, *130*, 7339−7344. (b) Appleton, A. L.; Brombosz, S. M.; Barlow, S.; Sears, J. S.; Bredas, J. L.; Marder, S. R.; Bunz, U. H. F. Effects of Electronegative Substitution on the Optical and Electronic Properties of Acenes and Diazaacenes. *Nat. Commun.* **2010**, *1*, 91.
(35) Miao, S.; Appleton, A. L.; Berger, N.; Barlow, S.; Marder, S. R.; Hardcastle, K. I.; Bunz, U. H. F. 6,13-Diethynyl-5,7,12,14-tetraazapentacene. *Chem.—Eur. J.* **2009**, *15*, 4990−4993.
(36) Biegger, P.; Tverskoy, O.; Rominger, F.; Bunz, U. H. Synthesis of Triptycene-Substituted Azapentacene and Azahexacene Derivatives. *Chem.—Eur. J.* **2016**, *22*, 16315−16322.
(37) Huang, W.; Qiu, M.; Yu, F.; Chen, J.; Li, X.; Wei, Q.; Xing, G.; Wu, B.; Chen, W.; Zhang, Q. Synthesis, Characterization and Singlet Fission Behaviors of Heteroatom-Doped Polycyclic Aromatic Hydrocarbons with (β, β) Connected Furan/Thiophene Ring. *Chem.—Eur. J.* **2023**, *29*, No. e2022039.

https://doi.org/10.1021/acsomega.3c04452
ACS Omega 2023, 8, 32931−32939